THE JOURNAL OF PHYSICAL CHEMISTRY A

© Copyright 2003 by the American Chemical Society VOLUME 107, NUMBER 5, FEBRUARY 6, 2003

ARTICLES

Velocity Distributions of SiF and SiF_2 in an SiF_4 Plasma Molecular Beam

Jianming Zhang, Keri L. Williams, and Ellen R. Fisher*

Department of Chemistry, Colorado State University, Fort Collins, Colorado 80523-1872

Received: May 14, 2002; In Final Form: December 2, 2002

Our imaging of radicals interacting with surfaces (IRIS) technique has been used to measure the velocity distributions of SiF and SiF_2 molecules in an effusive SiF_4 plasma molecular beam as a function of applied rf power. Modeling the kinetic data yields the corresponding translational temperatures Θ_T. The translational temperatures of both SiF and SiF_2 increase with radio frequency (rf) power, from 571 ± 180 K at 80 W to 869 ± 54 K at 200 W for SiF, and from 427 ± 65 K at 80 W to 557 ± 31 K at 200 W for SiF_2. These differences in Θ_T for SiF and SiF_2 indicate that the SiF_4 plasma is not in full thermal equilibrium. Possible mechanisms for the trend of increasing Θ_T with rf power are discussed by correlating SiF and SiF_2 velocities with relative gas-phase densities. In addition, the effects of Θ_T on the surface scatter coefficients for each molecule have also been addressed.

I. Introduction

Fluorosilane plasmas have been widely studied either as a fluorine source for Si etching or as a silicon source for deposition of Si-based materials. In 100% SiF_4 plasmas, etching of Si, SiO_2, and Si_3N_4 occurs readily, and F-atoms are consider the primary etchant in these systems.[1−3] Addition of one or more source gases to SiF_4 plasmas leads to deposition of a wide range of fluorinated Si materials, such as a-Si:F:H using SiF_4/H_2[4,5] and $SiF_4-SiH_4-H_2$ plasmas,[6] a-Si,Ge:F:H using $SiF_4-GeH_4-H_2$ plasmas,[7] a-SiC:F using $SiF_4-CH_4-H_2$[8] and SiF_4-CH_4 plasmas,[9] a-Si_xN_y:F using SiF_4/NH_3 plasmas,[10] and F−SiO_2 using SiF_4-O_2[11,12] and $SiF_4-O_2-H_2-He$ plasmas.[13,14] Although extensive studies have been reported on these fluorinated Si materials, most have focused on the deposited materials, whereas little work has been done to characterize the gas-phase reactions and gas−surface interactions. Thus, the molecular-level details of deposition mechanisms in these systems are not fully understood.

The roles of gas-phase radicals and gas−surface interactions in these processes are important to an understanding of the overall fluorosilane chemistry. In addition, the energetics of both gas-phase and gas−surface reactions are extremely important. The imaging of radicals interacting with surfaces (IRIS) technique[15,16] provides a unique way to examine many of these aspects of the overall plasma chemistry. IRIS combines plasma molecular beam techniques with spatially resolved laser-induced fluorescence (LIF) to study the state-specific reactivity of plasma-generated species during a plasma-processing event. We have used the IRIS technique to explore the surface reactivity of SiF and SiF_2 in SiF_4 and SiF_4/H_2 plasmas.[17−20] The effects of radio frequency (rf) power, H_2 dilution, gas flow rate, and ion bombardment on surface reactivity were explored in those studies. In present work, we extend our research to the energy dissipation in SiF_4 plasmas, specifically, the translational or kinetic energies of SiF and SiF_2 molecules.

Knowledge of energy partitioning between different species is important to an overall understanding of the chemistry occurring in low-temperature plasmas. Kinetic energy distributions of plasma species are, however, difficult to determine.[21]

* To whom correspondence should be addressed. E-mail: erfisher@lamar.colostate.edu.

10.1021/jp0212040 CCC: $25.00 © 2003 American Chemical Society
Published on Web 01/16/2003

IRIS not only allows us to obtain surface reactivity of radicals interacting with surfaces but can also be used to measure velocity distributions of radicals in the plasma molecular beam[22−24] and of those scattered off of surfaces.[25,26] The average translational velocity of radicals is determined by taking LIF images at different time delays after the laser excitation of the radicals and evaluating the spatial shift of the LIF images. This velocity can then be converted to a translational or kinetic temperature. We have reported that the translational temperature, Θ_T, of NH_2 radicals in NH_3 plasmas increases linearly with applied rf power P.[22,25] At $P = 45$ W, $\Theta_T \sim 520$ K, whereas the rotational temperature Θ_R of NH_2 was estimated to be somewhat lower, $\Theta_R \sim 340$ K. In tetraethoxysilane/O_2 plasmas, we observed that Θ_T was nearly twice as large as Θ_R for OH radicals and that Θ_T increased slightly with rf power.[23] Most recently, we measured both Θ_T and Θ_R for SiH in SiH_4 and Si_2H_6 plasmas and found Θ_R was also significantly lower than Θ_T.[22−24] In the SiH study, however, both Θ_T and Θ_R were found to be independent of P from 10 to 85 W. Such studies have allowed us to discern between different mechanisms for energy partitioning and for dissociation of feed gases. In the present work, we have measured Θ_T for SiF and SiF_2, with $P = 80$−200 W. These measurements for SiF and SiF_2 radicals in SiF_4 plasmas complement our previous studies of surface reactivity for these two species.

II. Experiment and Data Analysis

The IRIS apparatus has been described in detail previously.[16] A brief description of the instrument with respect to these experiments is given here. Feed gases enter at the rear of a glass reactor tube, 13.56 MHz rf power is applied through a matching network, and an inductively coupled plasma is produced. Expansion of the plasma through a series of collimating slits into a double differentially pumped high vacuum chamber generates an effusive molecular beam consisting of virtually all species present in the plasma. The velocities of radicals in the effusive molecular beam approximate the random velocities in the bulk plasma.[22] A tunable excimer-pumped (XeCl, 100 mJ/pulse, 100 Hz) dye laser system with Coumarin 120 intersects the plasma molecular beam at either 45° or 90° downstream from the plasma source and excites the radicals of interest. Both geometries were used for each molecule, with no significant difference in the resulting velocity values. In the present work, the experimental geometry for the reported data was 45° for the SiF data and 90° for the SiF_2 data. Spatially and temporarily resolved LIF signals are collected by an electronically gated, intensified charge coupled device (ICCD) located perpendicular to both the molecular beam and the laser beam, directly above the interaction region. "Snapshots" of the LIF images of the expanding molecular beam are taken at different camera gate delays after laser excitation. The velocity of the radicals can subsequently be deduced from the spatial shift in maximum intensity of the fluorescence between the different delays.

In the present work, SiF_4 (Matheson, 99.9%) is introduced into the plasma chamber at a flow rate of 30 sccm. The applied rf power P is varied from 80 to 200 W. The operating pressure in the plasma chamber varies from ∼110 mTorr for 80 W plasmas to ∼150 mTorr for 200 W plasmas. The molecular beam was collimated by two slits, ∼1.2 and ∼1.4 mm wide, with the second slit 12 mm downstream from the first one. For SiF velocity measurements, the laser was tuned to 437.348 nm (∼10mJ/pulse), corresponding to the 5.5 J-state of the (0,0) band of the SiF $A^2\Sigma^+ \rightarrow X^2\Pi$ electronic transition.[18] For SiF_2 velocity measurements, the laser was tuned to 221.530 nm (0.8 mJ/pulse) by frequency doubling the output of the dye laser, corresponding to the 2_0^4 vibronic band of the $A^1B_1 \rightarrow X^1A_1$ transition.[19]

To increase spatial and temporal resolution, the ICCD pixels are not binned and a short gate width of 100 ns is used. The ICCD images are taken at four different time delays, typically 160, 360, 560, and 760 ns after the laser pulse for SiF excitation, and 110, 510, 910, and 1310 ns after the laser pulse for SiF_2 excitation. For high accuracy of the measurements, time delays are preferentially taken as high as possible. However, this is limited by the radiative lifetime of SiF (∼230 ns[27]) and SiF_2 (variable lifetime from 60 ns to several μs[28]). In our experiment, the SiF_2 LIF signals decreased to a very low value at time delays longer than 2 μs. We have measured the decrease in SiF_2 LIF intensity as a function of time delay. Fitting the data using an exponential function yields a time decay constant of ∼250 ns. This value should be considered as a lower limit of the SiF_2 fluorescence lifetime since SiF_2 LIF signals can be detected at about twice the time delays used for SiF, which has a fluorescence lifetime of ∼230 ns.[27] LIF signals of 8 to 12 accumulations of 60,000 laser shots were taken at each time delay. Background images obtained with an off-resonance laser wavelength were subtracted from the data images. One-dimensional cross section plots were made by averaging over 100 rows (8.96 mm) of pixels perpendicular to the laser beam and plotting signal intensity as a function of distance away from the laser beam path. Because the laser intersects the molecular beam at a 45° angle, a conversion factor of 1.414 is used to give the final plot of LIF intensity as a function of distance along the molecular beam. This leads to "snapshots" of the spatial position of the LIF intensity at four different time delays.

Because only relatively short time delays could be used in these systems, the spatial movement at different time delays is not obvious. Therefore, to accurately determine the positions of LIF intensity peak position, a symmetrical laser spatial profile is assumed and the plot is fitted by a Gaussian function. As discussed in detail previously,[24] the peak positions are then plotted as a function of time delay and fit with a linear regression. The slope of this linear fit gives the average velocity of SiF or SiF_2 along the center axis of the molecular beam. This is considered a lower limit to the velocity because radicals are also moving in radial directions. To account for this, a Monte Carlo simulation program[22,25] is used to simulate the spatial LIF intensity of SiF and SiF_2 along the molecular beam's central axis. This model assumes a Gaussian laser beam profile and a Maxwell−Boltzmann distribution of molecular velocities in the molecular beam. The peak positions of the simulated data are plotted again as a function of time delay and the slope is compared with the experimentally obtained value. The procedure is repeated until a best fit is obtained, yielding the velocity and temperature of SiF and SiF_2 in the plasma. This method is very sensitive to small spatial shifts of the LIF peak position and thus is ideal for velocity measurement of radicals with relatively short radiative lifetimes. Indeed, we have successfully demonstrated the procedure in the measurement of the translational velocity of SiH radical (radiative lifetime of 534 ns[29]) in SiH_4 and Si_2H_6 plasmas.[24]

III. Results

A representative velocity measurement is shown in Figures 1 and 2 for SiF in a 100% SiF_4 plasma at $P = 200$ W, using four different time delays and a 45° geometry between the laser and the molecular beam. Figure 1 shows the ICCD images, and Figure 2 shows the corresponding cross-sectional LIF signals.

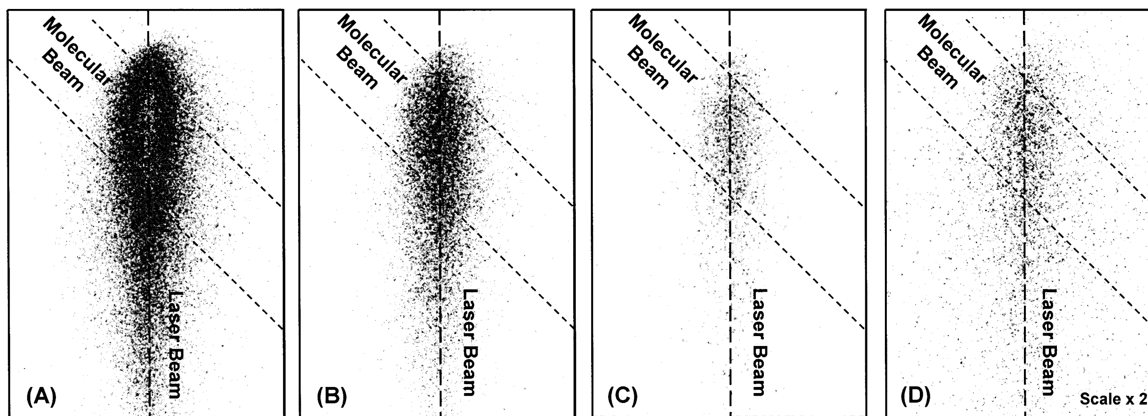

Figure 1. ICCD images of LIF signals for SiF radicals in a 100% SiF_4 plasma molecular beam ($P = 200$ W) at four different time delays: (A) 160 ns, (B) 360 ns, (C) 560 ns, and (D) 760 ns after laser excitation. The experimental geometry for these data was 45° between the laser and the molecular beam. Dashed lines indicate the locations of the molecular beam and the laser beam.

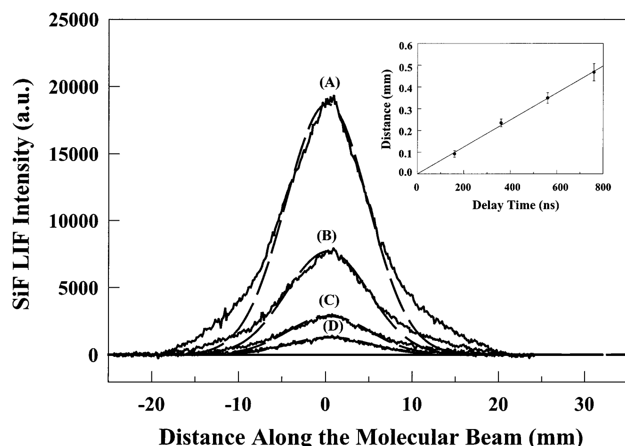

Figure 2. Cross sectional data for the SiF LIF images shown in Figure 1 (solid lines) at four different time delays: (A) 160 ns, (B) 360 ns, (C) 560 ns, and (D) 760 ns after laser excitation. Simulated results with an SiF translational temperature of 855 K are also shown (dashed lines). In the inset, the spatial positions of the maxima of the LIF signals are plotted as a function of time delay. The slope (617 m/s) of the linear regression corresponds to the velocity of the SiF radicals in the direction of the central axis of the molecular beam, which is a lower limit to the SiF velocity in the molecular beam.

As the time delay increases, the intensity of the LIF signal decreases and the cross sectional LIF signal shifts along the direction of the molecular beam. The shift is more clearly seen in the inset of Figure 2, which shows the peak position of LIF intensity as a function of time delay. The LIF intensity decreases with increasing time delay as a result of the radiative decay of the excited SiF $A^2\Sigma^+$ state after the laser excitation pulse. As noted above, larger steps in time delay are preferred for more accurate measurement, but this is limited here by the relatively low signal-to-noise ratio at longer time delays. The time delay steps (200 ns) are nearly as long as the radiative lifetime of SiF (230 ns).

The simulation results are also plotted in Figure 2. The good agreement between the experimental and simulated cross sections indicates the SiF radicals in the effusive molecular beam follow a Maxwell−Boltzmann distribution. The simulation yields an average velocity, v, of 621 ± 22 m/s, corresponding to $\Theta_T = 855 \pm 60$ K under these plasma conditions. ($\Theta_T = \pi m v^2/8k$, where m is the mass of the radical and k is Boltzmann constant).

Figure 3 shows the ICCD images of the velocity measurement for SiF_2 in a 100% SiF_4 plasma molecular beam at $P = 200$ W, taken with a 90° geometry. The corresponding cross-sectional LIF signals along with the simulation results are shown in Figure 4. Comparison of the experimental data and the simulation results gives an average SiF_2 velocity of 425 ± 14 m/s, corresponding to $\Theta_T = 565 \pm 37$ K. This is significantly lower than that found for SiF under the same plasma conditions.

TABLE 1: Translational Temperatures (K) of SiF and SiF_2 Radicals[a]

	rf power				
	80 W	100 W	130 W	170 W	200 W[b]
SiF	571 ± 180	598 ± 85	802 ± 88	831 ± 120	869 ± 54
SiF_2	427 ± 65	445 ± 1	457 ± 67	511 ± 18	557 ± 31

[a] Errors are determined from the linear regression analysis for the plots of LIF peak position as a function of time delay. These encompass four data sets for measurements made at the higher applied rf powers and 8−12 data sets for measurements made at the lower rf powers. [b] Data at 200W includes data taken at two different experimental geometries, 45° and 90°. Errors for these values were calculated using weighted averages.

Figure 5 show the average translational temperatures of SiF and SiF_2 radicals in SiF_4 plasmas as a function of applied rf power. These values and error limits are also listed in Table 1. As noted in the Experimental Section, we have measured the velocities of SiF and SiF_2 for $P = 200$ W at experimental geometries of both 45° and 90°, yielding identical results within experimental error. In Figure 5 and Table 1, the values for $P = 200$ W are the weighted average of these two experimental geometries. For SiF_2, the average translational temperatures increase linearly with rf power, with a slope of 0.946. For SiF, Θ_T also increases with rf power, but does so with a sharp increase in Θ_T between $P = 100$ W and $P = 130$ W. Interestingly, this rapid increase is concomitant with a transition of the SiF_4 plasma from low-density regime to high-density regime. This transition is characterized by a strong increase in light emission and electron density. Although some of the observed increase in kinetic temperature of the SiF_x species could be attributed to the increase in pressure at higher P, it does not account for the significant differences in Θ_T for the two species, the nonlinear behavior of the SiF data in Figure 5, or the increased dissociation and ionization in the plasma.

IV. Discussion

In two parallel studies of surface reactivity of SiF and SiF_2 in SiF_4 and SiF_4/H_2 plasmas,[18,19] we observed that the density of SiF_2 increased linearly with P, while the density of SiF

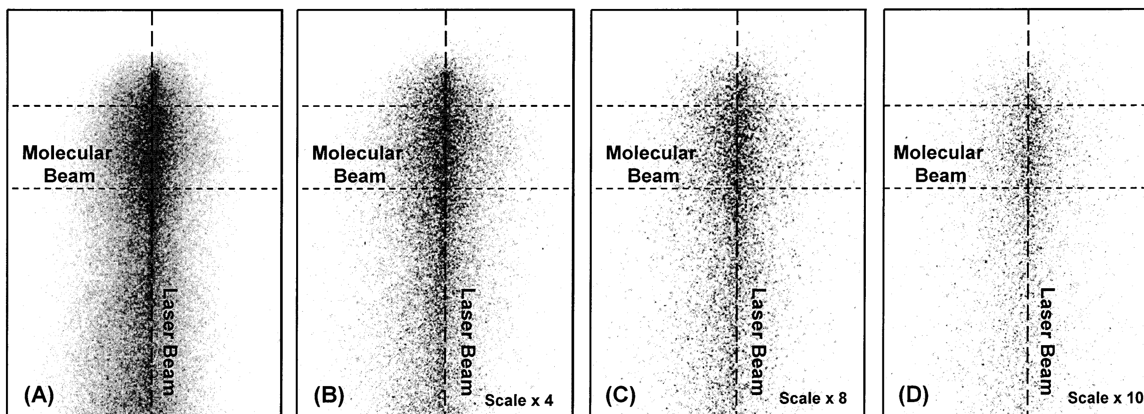

Figure 3. ICCD images of LIF signals for SiF_2 radicals in a 100% SiF_4 plasma molecular beam ($P = 200$ W) at four different time delays: (A) 110 ns, (B) 510 ns, (C) 910 ns, and (D) 1310 ns after laser excitation. The experimental geometry for these data was 90° between the laser and the molecular beam. Dashed lines indicate the locations of the molecular beam and the laser beam.

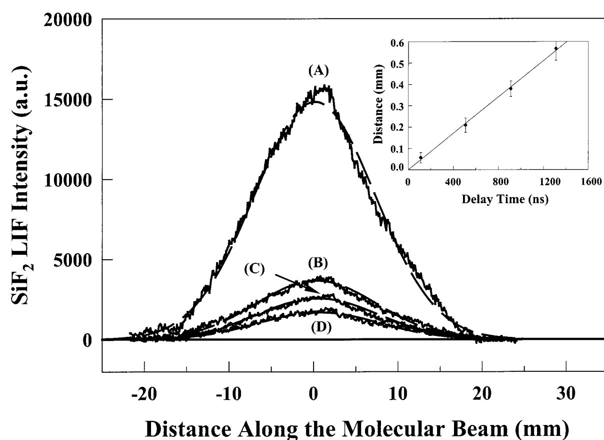

Figure 4. Cross sectional data for the SiF_2 LIF images shown in Figure 3 (solid lines) at four different time delays: (A) 110 ns, (B) 510 ns, (C) 910 ns, and (D) 1310 ns after laser excitation. Simulated results with an SiF_2 translational temperature of 565 K are also shown (dashed lines). In the inset, the spatial positions of the maxima of the LIF signals are plotted as a function of time delay. The slope (423 m/s) of the linear regression corresponds to the velocity of the SiF_2 radicals in the direction of the central axis of the molecular beam, which is a lower limit to the SiF_2 velocity in the molecular beam.

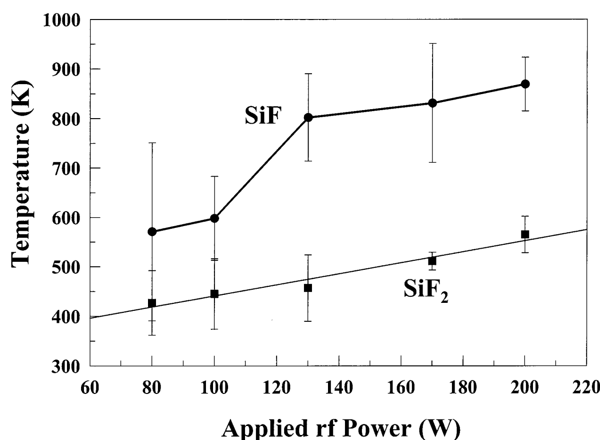

Figure 5. The average translational temperatures of SiF (circles) and SiF_2 (squares) radicals in SiF_4 plasmas as a function of applied rf power. The straight line for SiF_2 data represents a linear regression fit to the data with a slope of 0.946 and an r^2 value of 0.976.

increased slowly with rf power up to ~100 W and then increased rapidly above 100 W. This same dependence of SiF density on applied rf power was also observed in our study of SiF radicals in SiF_4 plasmas using resonance enhanced multiphoton ionization combined with time-of-flight mass spectrometry (REMPI-TOFMS).[30] The observation that both velocities and densities of SiF and SiF_2 increase with increasing power dependence indicates that the rf power contributes to the dissociation of SiF_4 and that at least part of the increased power is partitioned into translational heating of the SiF and SiF_2 radicals. Furthermore, the similarity in the power dependencies of the velocities and densities suggests that the translational heating of SiF and SiF_2 radicals is related to the number densities of these two species

In SiF_4 plasmas, SiF_x ($x = 0, 3$) radicals or ions are produced by electron-induced dissociation of SiF_4. The loss of F atoms could be either stepwise or nearly simultaneous, in a concerted fashion. The products can be either ground state or excited state, neutral or ionic. Bruno et al.[5] observed that excited SiF_x^* ($x = 1-3$) species are mainly generated by a direct electron impact excitation process of the same species, i.e., $SiF_x + e^- \rightarrow SiF_x^*$. When rf power is increased, the number densities of SiF and SiF_2 radicals and electrons density increases, which also leads to increased number density of excited SiF^* and SiF_2^*. This is consistent with the fast increase of light emission during the low-density to high-density transition in our system when the rf power is increased from 100 to 130 W. The processes that create the excited SiF^* and SiF_2^* species could also contribute to translational heating of SiF and SiF_2 molecules. This can happen in two ways. Collisional relaxation of the excited SiF_x species could result in ground-state SiF_x that have higher kinetic energy. Alternatively, the SiF_x^* species could transfer their excess energy in a collision with other SiF_x molecules, converting this energy to translational energy of the products (i.e., SiF or SiF_2).[31] This heating is likely responsible for the similarity in the power dependence of SiF and SiF_2 velocities and number density, as well as for the rapid increase of Θ_T of SiF during the low-density to high-density transition.

Other translational heating processes, such as collisions with energetic ions, are also related to the radical density and electron density of the plasma. Increasing the rf power increases the ion density, energy, and collision frequency of ions and radicals.[21] If the same ionic or neutral species collides with SiF and SiF_2, the SiF will have higher translational velocity than the SiF_2 because of the difference in mass. This may account for the observation that SiF has a higher translational temperature than SiF_2 at all rf powers. The difference in Θ_T of SiF and SiF_2 radicals, however, could be the result of the dynamical history of the dissociation processes of SiF_4, in which lighter fragments carry away more energy.

Knowledge of energy partitioning between different species is important to developing a complete understanding of the chemistry of low-temperature plasmas. The translational energy distributions of SiF and SiF_2 radicals in SiF_4 plasma as a function of rf power also provide insights into the interactions of these two species with surfaces. In two parallel studies, we have explored the surface reactivity of SiF and SiF_2 in SiF_4 and SiF_4/H_2 plasmas and the effects of rf power, H_2 dilution, gas flow rate, ion bombardment, and substrate temperature.[17−20] In these studies, we have measured scattering coefficients S [the fraction of radicals scattering from the surface relative to those in the molecular beam] for both SiF and SiF_2 as a function of both rf power and substrate temperature. For both molecules, S increases significantly with increasing rf power. Mullins and co-workers have shown that when an Ar atom collides with a surface, the trapping probability for the atom on the surface decreases with increasing kinetic energy of the incident Ar.[32] Although not as simple as Ar atoms, we can draw a parallel to this with our results for SiF and SiF_2. As P increases, Θ_T for both SiF and SiF_2 increase. Thus, the trapping probabilities of SiF and SiF_2 should decrease, consistent with the observations that the S values for SiF and SiF_2 increase with rf power.

As a final remark, for low-pressure discharges, such as the type of inductively coupled plasma studied here, the plasma is commonly not in thermal equilibrium.[21] The rotational temperature of SiF Θ_R has been determined to be about 450 ± 50 K for 40−170 W rf power,[18] which is independent of rf power and significantly lower than the Θ_T for SiF measured under the same conditions. This phenomenon, that rotational temperature is lower than translational temperature of the same species, has been observed for other species we have studied with IRIS. Specifically, they are NH_2 in an NH_3 plasma,[25] OH radicals in a tetraethoxysilane/O_2 plasma,[23] and SiH radicals in SiH_4 and Si_2H_6 plasmas.[24] In SiF_4 plasmas, the rf energy is dissipated into the dissociation of SiF_4 molecules and the vibrational, rotational, and translational motion of the fragments. The initially formed SiF and SiF_2 radicals might be rotationally and/or vibrationally hot and subsequent collisional quenching may transfer this energy to translational energy. On the basis of the common assumption that the average rotational temperature of the gas-phase species is equal to the ambient gas temperature,[32] we estimate that the average gas temperature in our SiF_4 plasma is ∼400K at $P = 20-80$ W. The difference between rotational temperature and translational temperature for SiF and the difference between translational temperatures of SiF and SiF_2 indicate that the species in SiF_4 plasmas are not fully in thermal equilibrium.

V. Summary

The SiF and SiF_2 velocities in the SiF_4 plasma molecular beam have been measured as a function of applied rf power using the IRIS technique. Modeling the velocity data yields the transitional temperatures of SiF and SiF_2 in the plasma, which increase with increasing rf power. This trend is correlated to the radical number density for both species in the plasma. Moreover, Θ_T for SiF is higher than that of SiF_2 for the same rf power, which indicates that the SiF_4 plasma is not in full thermal equilibrium. Possible effects of translational temperature changes on scatter coefficients have also been addressed in terms of simple scattering probability. These are more fully discussed in our studies of the surface interactions of SiF and SiF_2.[17−20]

Acknowledgment. This work is supported by the National Science Foundation (Grants NSF 9812332 and NSF 0137664) and the Dreyfus foundation. We also thank Prof. Elliot Bernstein for helpful discussions.

References and Notes

(1) Okada, Y.; Wagner, S. *Mater. Res. Soc. Symp. Proc.* **1990**, *192*, 541.
(2) Sparks, D. R. *J. Electrochem. Soc.* **1992**, *139*, 1736.
(3) Boyd, H.; Tang, M. S. *Solid State Technol.* **1979**, *12*, 133.
(4) Mutsukura, N.; Ohuchi, M.; Satoh, S.; Machi, Y. *Thin Solid Films* **1983**, *109*, 47.
(5) Bruno, G.; Capezzuto, P.; Cicala, G. *J. Appl. Phys.* **1991**, *69*, 7256.
(6) Kakinuma, H.; Mohri, M.; Tsuruoka, T. *J. Appl. Phys.* **1994**, *77*, 646.
(7) Bruno, G.; Capezzuto, P.; Cicala, G.; Cramarossa, F. *J. Mater. Res.* **1989**, *4*, 366.
(8) Cicala, G.; Bruno, G.; Capezzuto, P. *J. Vac. Sci. Technol. A* **1998**, *16*, 2762.
(9) Cicala, G.; Capezzuto, P.; Bruno, G.; Rossi, M. C. *Appl. Surf. Sci.* **2001**, *184*, 66.
(10) Gomez-Aleixandre, C.; Sanchez, O.; Albella, J. *Mater. Res. Soc. Symp. Proc.* **1991**, *190*, 107.
(11) Han, S. M.; Aydil, E. S. *J. Vac. Sci. Technol. A* **1997**, *15*, 2893.
(12) Lee, S.; Park, J. *J. Electrochem. Soc.* **1999**, *146*, 697.
(13) Alonso, J. C.; Pichardo, E.; Pankov, V.; Ortiz, A. *J. Vac. Sci. Technol. A* **2000**, *18*, 2827.
(14) Pankov, V.; Alonso, J. C.; Ortiz, A. *J. Vac. Sci. Technol. A* **1999**, *17*, 3166.
(15) Fisher, E. R.; Ho, P.; Breiland, W. G.; Buss, R. J. *J. Chem. Phys.* **1992**, *96*, 9855.
(16) McCurdy, P. R.; Bogart, K. H. A.; Dalleska, N. F.; Fisher, E. R. *Rev. Sci. Instrum.* **1997**, *68*, 1684.
(17) Williams, K. L.; Martin, I. T.; Fisher, E. R. *J. Am. Soc. Mass. Spectrom.* **2002**, *13*, 518.
(18) Williams, K. L.; Butoi, C. I.; Fisher, E. R. *J. Vac. Sci. Technol. A*. In preparation.
(19) Williams, K. L.; Fisher, E. R. *J. Vac. Sci. Technol. A*. Submitted for publication.
(20) Fisher, E. R. *Plasma Sources Sci. Technol.* **2002**, *11*, A105.
(21) Lieberman, M. A.; Lichtenberg, A. J. *Principles of Plasma Discharges and Material Processing*; Wiley and Sons: New York, 1994.
(22) McCurdy, P. R.; Venturo, V. A.; Fisher, E. R. *Chem. Phys. Lett.* **1997**, *274*, 120.
(23) Bogart, K. H. A.; Cushing, J. P.; Fisher, E. R. *J. Phys. Chem. B* **1997**, *101*, 10016.
(24) Kessels, W. M. M.; McCurdy, P. R.; Williams, K. L.; Barker, G. R.; Venturo, V. A.; Fisher, E. R. *J. Phys. Chem. B* **2002**, *106*, 2680.
(25) McCurdy, P. R.; Butoi, C. I.; Williams, K. L.; Fisher, E. R. *J. Phys. Chem. B* **1999**, *103*, 6919.
(26) Butoi, C. I.; Steen, M. L.; Peers, J. R. D.; Fisher, E. R. *J. Phys. Chem. B* **2001**, *105*, 5957.
(27) Davis, S. J.; Hadley, S. G. *Phys. Rev. A* **1976**, *14*, 1146.
(28) Stanton, A. C.; Freedman, A.; Wormhoudt, J. *Chem. Phys. Lett.* **1985**, *122*, 190.
(29) Bauer, H.; Becker, K. H.; Duren, R.; Hubrich, C.; Meuser, R. *Chem. Phys. Lett.* **1984**, *108*, 560.
(30) Williams, K. L.; Bray, J. A.; Venturo, V. A.; Fisher, E. R. *Chem. Phys. Lett.* **2000**, *323*, 137.
(31) Levine, R. D.; Bernstein, R. B. *Molecular Reaction Dynamics and Chemical Reactivity*; Oxford University Press: New York, 1987.
(32) Mullins, C. B.; Rettner, C. T.; Auerbach, D. J. *Chem. Phys. Lett.* **1989**, *163*, 111.